Solute Redistribution in Heavy-Ion Bombarded Copper Base Alloys

R.W. Knoll, P. Wilkes, G.L. Kulcinski

October 1980

UWFDM-383

FUSION TECHNOLOGY INSTITUTE

UNIVERSITY OF WISCONSIN

MADISON WISCONSIN

Solute Redistribution in Heavy-Ion Bombarded Copper Base Alloys

R.W. Knoll, P. Wilkes, G.L. Kulcinski

Fusion Technology Institute
University of Wisconsin
1500 Engineering Drive
Madison, WI 53706

http://fti.neep.wisc.edu

October 1980

UWFDM-383

Solute Redistribution in Heavy-Ion Bombarded Copper Base Alloys

R. W. Knoll, P. Wilkes*, and G. L. Kulcinski

Fusion Engineering Program
Nuclear Engineering Department
University of Wisconsin
Madison, WI 53706

October 1980

UWFDM-383

Presented at the Fall 1980 Meeting of The Metals Society of the AIME, Oct. 5-9, Pittsburgh, PA.

---

*Now at Elmbrook Church, Waukesha, Wisconsin.

ABSTRACT

The redistribution of solute atoms near the surfaces of ion-bombarded Cu-base alloys (Cu-3.4 at% Be, Cu-1 at% Co, and Cu-1 at% Fe) has been measured using Auger electron spectroscopy combined with sputtering. Solution annealed alloy specimens were irradiated with 14 MeV Cu ions at temperatures of 350°C to 475°C, to doses of 8.8×10^{14} - 3.5×10^{16} ions/cm^2 (0.06 to 2.7 dpa at the specimen surfaces). Strong irradiation induced surface segregation of the undersize Be solute was observed, which increased with irradiation temperature and dose. Some Be surface segregation also occurred in unirradiated control samples, so the degree of segregation in irradiated Cu-Be depended upon the thermal history of the specimen. The Co and Fe solutes, which are similar in atomic size to Cu, underwent little or no redistribution during irradiation. Irradiation induced precipitation in the Cu-Be was observed by electron microscopy, although these results are discussed only briefly in this paper.

1. Introduction

In recent years, considerable effort has been devoted to the experimental measurement of solute enrichment or depletion near point-defect sinks in irradiated alloys [1-14]. The understanding of such localized changes in the alloy composition is important, since these changes could alter the physical properties of the bulk material. The origin of radiation induced solute redistribution is linked to an interaction between the alloying elements and radiation induced point-defect currents migrating to sinks [15-16]. The magnitude and type of redistribution (enrichment or depletion) that occurs near a sink is related to the relative size of the solute atom, which governs the strain field surrounding the atom [17,10]. Regions near sinks tend to become enriched with undersize solutes and depleted of oversize solutes. Although solute segregation has been observed near internal sinks such as voids [1-5] and dislocations [6], many measurements have been performed near the external surfaces of irradiated specimens [7-14], because the free surface is an unsaturable point-defect sink, and is easily accessible to the experimenter.

While many previous solute segregation experiments have focussed on Ni-base alloys [5,7-10,12-14], little attention has been paid to other fcc metals. The present paper reports on measurements of solute concentration profiles near the surfaces of several Cu-base alloys that have been irradiated with 14 MeV Cu ions at temperatures between 350°C-475°C, to doses ranging from 0.08 dpa to 3.5 dpa at the surface. Measurements reported here, which were made using Auger electron spectroscopy (AES) combined with sputtering, are part of an on-going investigation of solute redistribution and phase stability in irradiated Cu-base alloys.

2. Experimental Methods

The alloys used in this experiment were Cu-3.4 at % Be, Cu-1 at % Co and Cu-1 at % Fe. Beryllium, a very undersize solute in copper, has a relative volumetric size factor [18] of -26.5%; Co is slightly undersize, with a size factor of -3.78%. The Fe solute is believed to be slightly oversize, although there is disagreement on this point (see Discussion). The Cu-1 at % Co and Cu-1 at % Fe alloys were prepared by Materials Research Corporation using MARZ grade stock with a nominal impurity content of less than 20 ppm. The Cu-3.4 at % Be (1/2 wt % Be) alloy was prepared by Wilkes [19]. This alloy contained ~ 550 ppm impurities, mainly Mg, Fe, Sn and Si. Portions of the alloy stock were rolled into 0.25 mm - 0.38 mm foils, from which specimens ~ 1 cm x 1 cm were cut.

All specimens were annealed and solution treated in an H_2 atmosphere at 800°C-900°C for ~ 1-1/2 hrs, then quenched into distilled water. The Cu-Be foils were mechanically polished after the anneal. Before loading into the irradiation target chamber, ~ 25 μm - 50 μm was electropolished from each specimen to provide a clean surface.

The alloy specimens were irradiated with 14 MeV Cu^{+3} ions in the Heavy Ion Irradiation Facility of the University of Wisconsin tandem Van de Graaff accelerator. This facility has been described in detail previously [20]. The principal modification to this system for the present experiments has been redesign of the specimen holder and furnace assembly. In the original design, specimens were mounted adjacent to each other and were effectively heated en masse, so the temperature history of an individual specimen could not be controlled. Specimens in the redesigned holder were thermally isolated from one another, which allowed an individual sample to be heated only during its

irradiation. Some specimens were irradiated in the old holder, where they were subjected to annealing before and after irradiation, as discussed later.

Vacuum pressures during irradiation were generally less than 2×10^{-7} torr, the residual gas composed mainly of hydrogen. Irradiation temperatures were monitored by thermocouples mounted behind and in good thermal contact with each foil. A 3 mm diameter mask-aperture located in front of the sample defined the shape and position of the heavy ion beam striking the sample.

The damage energy distribution for 14 MeV Cu on Cu was generated using the Brice codes COREL, RASE 4 and DAMG 2 [21], then converted into displacements-per-atom (dpa) vs. depth using a mean displacement energy of 34 eV. The dpa curve corresponding to an ion flux of 1×10^{16} ions/cm^2 is shown in Fig. 1. Effects of the alloying elements on the ion energy loss were not considered in these calculations. The peak damage occurred at a depth of ~ 2300 nm into the target and was ~ 16 times greater than the damage at the target surface. Since all AES measurements were made within ~ 300 nm of the specimen surface, dpa damage levels quoted in this paper are those at the surface rather than at the damage peak. In this experiment, the dpa rates at the specimen surface ranged between 1.7×10^{-4} dpa/sec and 3.0×10^{-4} dpa/sec.

The alloy composition near the irradiated foil surface was profiled using a Physical Electronics Industries Model 548 Auger/ESCA System. A 3 keV primary electron beam of 30 μA, with a diameter of ~ 0.2 mm, excited the Auger transitions. Sputtering was accomplished with a beam of 2 keV Xe^+ or 5 keV Ar^+ ions. The sputtering rates were determined by masking off part of the specimen close to the point of contact of the primary electron beam, then measuring the resulting step-height with an interference microscope. These rates were assumed to be linear, i.e., no corrections were made for changes in

alloy composition with depth. Absolute sputtering rates were also measured by clocking the time required to sputter through a foil of known thickness, while simultaneously monitoring the Auger spectrum from the foil. Pressures in the high vacuum chamber were $\sim 10^{-9}$ torr before sputtering began, and $\sim 5.5 \times 10^{-5}$ torr after introduction of the high purity Xe or Ar.

The energy spectra of the Auger electrons were recorded as dN(E)/dE vs. E, where E is the energy of the Auger electron and N(E) is the number of electrons detected at that energy. The concentration of an element is related to the peak-to-peak amplitude of dN/dE for an Auger transition characteristic of that element. The composition vs. depth measurements in the Cu-Be specimens were obtained by simultaneously sputtering and measuring the amplitudes of selected Auger peaks, with the instrument in a multiplex mode. Auger spectra were also recorded before sputtering began and following the completion of sputtering. In the Cu-Co and Cu-Fe samples, the measurements were made by sputtering, then intermittently recording the Auger spectra with the ion beam off.

Following Auger analysis, all specimens were thinned and studied in the electron microscope, to determine the effects of irradiation on precipitation in the damage zone. These results are discussed very briefly in this paper.

3. Results

Depth profiles of the relative alloy composition near the irradiated surfaces of Cu-3.4 at % Be samples are shown in Figs. 3-7. The relative solute concentration profiles in Cu-1% Co and Cu-1% Fe are shown in Figs. 9 and 10, respectively. Composition profiles labeled "control" were measured from areas of the foil masked from the Cu ion beam, whose temperature history was identical to that of the irradiated spot. Irradiation temperatures and

heavy-ion doses (which can be converted to dpa using Fig. 1), are given in each figure.

In the Cu-Be specimens, the relative concentration of an element at a given depth was assumed to be proportional to the peak-to-peak Auger amplitude of that element, after correction for the element's relative Auger sensitivity. The elemental sensitivity factors and the method of calculation are from Davis, et al. [22]. However, the concentration profiles presented here should be considered only first order approximations. The data are presented in this manner to facilitate comparison between specimens. Accurate quantitative analysis would have required the use of Cu-Be standards and more detailed calculations to determine the relative sensitivity factors of the elements [23,24]. Without the use of standards of various compositions, matrix effects on the Auger signals are not well known. The relative beryllium concentration was measured using the Auger transition at ~ 95 eV. The transitions at 508 eV (oxygen) and 920 eV (copper) were also used in the calculations.

A typical Auger spectrum of the surface of an irradiated foil, along with a spectrum from a depth of ~ 100 nm, are given in Fig. 2. The upper spectrum in this figure contains a beryllium peak at 95 eV and also a large oxygen peak at 508 eV. Before describing the results of the Be measurements, these two features must be discussed. The main Auger peak for pure, or chemically unbound beryllium, is reported to occur at 104 eV rather than 95 eV [22,25]. Previous AES studies on both pure Be [25] and on a Cu-2% Be alloy [26] indicated that the 94 eV - 96 eV peak is characteristic of oxidized beryllium. The effect of Cu alone on the energy and yield of the Be Auger electrons is not known, since no spectra from clean Cu-Be were found in the literature. In this experiment, Be giving rise to a 104 eV signal would have gone undetected

because of interference with the 105 eV peak of Cu. Therefore, the question of whether the 95 eV peak was representative of the actual Be concentration was investigated.

As shown in Fig. 6, the ratio of the oxygen/beryllium concentrations typically decreased with depth. To check if any unoxidized Be existed that did not contribute to the 95 eV peak, the following test was performed. A specimen irradiated at 430°C (not shown in these figures), which exhibited a large Be enrichment near the surface, was sputtered until the 95 eV peak decreased to ~ 25% of its initial value. The specimen was then withdrawn from the high vacuum chamber to the reaction chamber of the instrument, where it was exposed to air for ~ 5 minutes. A scan of the freshly oxidized specimen, after re-insertion to the same position within the high vacuum chamber as before, showed an increase in the 508 eV oxygen peak as expected, but no increase in the 95 eV Be peak. The peak height of the beryllium transition at 95 eV was therefore assumed to represent the actual beryllium concentration.

Each Cu-Be specimen in Figs. 3-6 was held at the indicated temperature only while it was exposed to the heavy ion beam. Otherwise the specimen remained at temperatures between 100°C-200°C, until irradiation of all specimens in the target chamber was completed. Strong beryllium enrichment occurred near the surfaces of all irradiated foils. However, significant beryllium enrichment due to thermal segregation was also observed in all control specimens.

The relative concentrations of Be, Cu and O vs. depth in a specimen irradiated at 475°C with 1.8×10^{16} ions/cm^2 (1.35 surface dpa) are shown in Fig. 3. The amplitude of the Be Auger peak within ~ 15 nm of the surface is about 30 times greater than the Be amplitude at a depth of ~ 100 nm, where the

profile levels off. Error bars on the data in this figure represent the typical estimated uncertainty in the measured peak-to-peak Auger amplitudes due to random instrument noise. At depths greater than ~ 60 nm the relative uncertainty in the Be concentration becomes quite large due to the small amplitude of the Be Auger peak. No attempt was made to measure Be concentrations at depths beyond the enriched zone, where Be depletion must have occurred due to conservation of solute.

In Fig. 4 the Be concentration profile of the 475°C specimen is compared with Be profiles in several other specimens irradiated at lower temperatures, but with similar ion doses. Beryllium concentration profiles from corresponding control samples are also shown in Fig. 4. There is a striking difference between the Be profiles in the samples irradiated at 475°C and 375°C to a surface dose of ~ 1.3 dpa. The maximum Be concentration is about 40% higher in the 475°C sample, while the width of the beryllium enriched zone is ~ 400% greater. The maximum Be enrichment is lower still in the 350°C specimen, which was irradiated to twice the dose of the higher temperature samples. The widths of the enriched zones in the 350°C and 375°C samples are similar. In the control samples, both the maximum Be concentration and the width of the enriched zone decrease with temperature. An abrupt decline in the Be concentration profiles begins at the surface of the control samples, whereas in the irradiated specimens the Be concentration remains approximately constant in the first 10-20 nm, then drops sharply.

In Figs. 5 and 6 the relative Be concentration profiles are plotted vs. depth for specimens irradiated at 375°C-430°C, but to lower doses than in Fig. 4. While the shapes and maximum values of the Be profiles are about the same, the width of the solute enriched region decreases with decreasing dose and

irradiation temperature. The damage levels at the surfaces of these specimens ranged from 0.08 dpa to 0.33 dpa. As in the higher dose specimens, Be enrichment in the control samples is substantially smaller than in the irradiated samples, and the Be concentration decreases approximately linearly with depth.

The effect of pre-irradiation and post-irradiation aging on the near-surface Be enrichment in several Cu-Be foils is shown in Fig. 7. Beryllium concentration profiles labeled "AGED" are from samples that were held at temperatures between ~ 475°C-350°C, for various lengths of time, before and after irradiation to 0.2 surface dpa at the temperatures indicated in the figure. The 475°C specimen was held at ~ 475°C for 6 hours before irradiation, then at 430°C to 350°C for ~ 8 hours after irradiation. The 430°C specimen was annealed at 475°C-430°C for ~ 9 hours before irradiation, and at 400°C-350°C for 5 hours after irradiation. Finally, the temperature of the 350°C specimen ranged from 475°C-350°C for ~ 14 hours before irradiation. This unusual heat treatment was not intentional, but resulted from the design of the specimen holder used for these samples, as explained earlier. The purpose of including these concentration profiles is to illustrate the sensitivity of the beryllium enrichment to the thermal history of the specimen. The Be enrichment in the aged control sample is much less than in the aged irradiated specimens, yet larger in amplitude and width than profiles in control samples in Figs. 4-6. Several Be concentration profiles from specimens that were heated during irradiation only are also plotted in Fig. 7, for comparison with the aged specimens.

Although Auger analysis was performed only to depths within ~ 100 nm of the surface of the Cu-Be foils, the alloy microstructure deeper in the foils was studied by transmission electron microscopy (TEM). Platelike precipitates

(belived to be γ'CuBe) were observed in all Cu-Be specimens irradiated at 375°C-430°C, and in high dose specimens irradiated at 475°C. No precipitation occurred in any of the unirradiated control specimens. As an example, Fig. 8 shows precipitation throughout the damage zone of a specimen that was irradiated at 430°C with 3.2×10^{15} ions/cm^2, then thinned in cross section. Note the absence of precipitation beyond the end-of-range of the incident ions.

The relative concentrations of cobalt vs. depth in Cu-1% Co foils irradiated at 475°C and 400°C are plotted in Fig. 9. Since the peak height of the Co Auger transition was always much smaller than the peak height of the Cu transition, and since Co and Cu were the only elements present in the samples, the Co concentration is represented by the ratio of the Co (656 eV) to Cu (920 eV) peaks. The largest Co Auger peak, at 775 eV, was not used because of interference with the 776 eV peak of copper. Error bars on the data in Fig. 8 represent uncertainty in measurement of the small Co peak due to random instrument noise. The data from the 400°C unirradiated control sample are typical of all control samples measured. These specimens were irradiated to surface doses of ~ 0.25 dpa (at 475°C and 400°C) and ~ 1.1 dpa (at 475°C). As Fig. 8 indicates, no solute redistribution occurred in the Cu-Co specimens, within the limits of experimental error (~ ± 30%).

Concentration profiles of Fe in irradiated Cu-1% Fe samples, obtained from the measured ratios of the Fe (651 eV) to Cu (920 eV) Auger peak heights, are plotted in Fig. 10. Again, the relatively small signal to noise ratio results in a large uncertainty in the measured Fe peak height. Within the limits of the estimated experimental error the Fe concentration is approximately constant with depth in samples irradiated at 350°C and 400°C to ~ 0.76 surface dpa, and in the 400°C control sample. However, the Fe concentration

in the specimen irradiated at 450°C (0.76 surface dpa) is partially depleted within ~ 150 nm of the free surface. The Fe/Cu ratio at the surface of the specimens was not measureable because oxygen and carbon surface contamination reduced the relative size of the Fe Auger peak to the level of the background noise.

4. Discussion

4.1 Behavior of Beryllium Solute

The enrichment of Be near the surface of irradiated Cu-3.4 at % Be foils, estimated by the area under the Be concentration-vs.-depth curves, was in all cases greater than in corresponding unirradiated samples. This enrichment increased with both irradiation temperature and dose (Figs. 3-6). Examination of relatively low dose specimens (0.08 suface dpa) irradiated at 430°C and 400°C in Figs. 5 and 6 shows a very rapid build-up of Be at the foil surface, to a maximum value of roughly 50% Be. Irradiation to higher doses, at temperatures $\lesssim$ 430°C, increased the width of the Be enriched zone, but did not significantly alter this maximum Be concentration. The effect of increasing the irradiation temperature, within the temperature range used in this study (350°C-475°C), was to increase both the width of the Be enriched region and the concentration of Be within this region (Fig. 4).

The shape of the Be concentration vs. depth profiles in all irradiated specimens (a relatively flat profile within 5-15 nm of the surface followed by a steep gradient) is assumed to indicate a precipitate layer near the surface. Although the microstructure of this region was not examined by TEM, the evidence of irradition induced precipitation deeper in the damaged region (Fig. 8) supports this assumption.

The Be enrichment due to thermal segregation only, which occurred in unirradiated regions of the foils, increased with temperature, and increased with the length of time the specimen was held at high temperature. Segregation of Be to the surface of Cu-Be samples during heating has been also noted by previous investigators [11,26,27], who assumed that oxidation stabilized the Be. The surface segregation of Be during heating before irradiation is believed to be the cause of the large Be near-surface enrichment observed in the aged specimen in Fig. 7.

Segregation of the undersize Be solute to the surface during irradiation agrees with the results of previous solute segregation studies in Ni alloys containing undersize solutes [7,9-13]. The irradiation induced Be segregation observed here is consistent with the work of Bartels, et al. [28], who observed a decrease in the amount of Be in solution in very dilute Cu-Be alloys, following 3 MeV electron irradiation. Presumably the Be segregated to internal sinks. In those studies, the segregation mechanism was assumed to be preferential transport of the undersize solute via the interstitial flux to sinks. This mechanism is assumed to operate in the present study, although radiation enhanced diffusion may also accelerate the transport of Be to the surface. Post-irradiation annealing studies will be done in the future to try to define the mechanisms responsible for the segregation.

4.2 Behavior of Co and Fe

According to theory [17,10], the magnitude and direction of solute segregation depends in part on the misfit between the solute and solvent atoms. The absence of significant radiation induced solute segregation in the Cu-Co alloy indicates little interaction between the Co atoms and the point defect

currents, which is consistent with the fact that Co and Cu atoms are similar in size.

In Cu-Fe, the depletion of Fe near the irradiated surface, at 450°C, would indicate a preferential exchange of oversize Fe atoms with vacancies, causing migration of the Fe atoms away from the surface [10]. The data in the present work, however, conflict with a recent HVEM study by Takeyama, et al. [29,30], who measured Fe enrichment near internal sinks (voids and grain boundaries) in Cu-2% Fe irradiated to 10 dpa at 300°C. Takeyama, et al. state Fe is an undersize solute in Cu, and therefore attribute the Fe enrichment to the interstitial transport mechanism proposed by Okamoto and Wiedersich [17]. A review of the literature reveals disagreement over whether Fe is oversize or undersize in Cu solid solution. Several x-ray studies [31,32] and a simple calculation [33] indicated Fe is slightly undersize, while other precision x-ray measurements [34,35] showed that the addition of Fe to pure Cu increased the lattice parameter of the solution. Because of this uncertainty in the size factor of Fe, the mechanism by which Fe segregates during irradiation cannot be determined at this time.

Acknowledgments

This work was supported by the U.S. Department of Energy under contract DE-AS02-78ET-52019. The authors are grateful to the following: the U.W. Nuclear Physics Group for use of the tandem accelerator; Dr. J. H. Billen for assistance in the irradiations; Dr. N. Tran for assistance in the Auger analysis, and Ms. E. A. Brown for typing the manuscript.

References

1. P. R. Okamoto, S. D. Harkness, and J. J. Laidler, ANS Transactions 16 (1973), 70.

2. P. R. Okamoto, A. T. Santhanam, H. Wiedersich, and A. Taylor, Nuc. Tech. 22 (1974), 45-51.

3. K. Farrell, J. Bentley, D. N. Braski, Scripta Met. 11 (1977), 243-248.

4. R. A. Erck, D. I. Potter, H. Wiedersich, J. Nuc. Mat. 80 (1979), 120-125.

5. A. D. Marwick, W. A. D. Kennedy, D. J. Mazey, and J. A. Hudson, Scripta. Met. 12 (1978), 1015-1020.

6. E. A. Kenik, Scripta Met. 10 (1976), 733-738.

7. D. I. Potter, L. E. Rehn, P. R. Okamoto, and H. Wiedersich, Scripta. Met. 11 (1977), 1095-1099.

8. A. D. Marwick and R. C. Piller, Rad. Effects 33 (1977), 245-250.

9. R. C. Piller and A. D. Marwick, J. Nuc. Mat. 71 (1978), 309-313.

10. L. E. Rehn, P. R. Okamoto, D. I. Potter, and H. Wiedersich, J. Nuc. Mat. 74 (1978), 242-251.

11. P. P. Pronko, P. R. Okamoto, and H. Wiedersich, Nucl. Inst. and Methods 149 (1978), 77-82.

12. L. E. Rehn, P. R. Okamoto, and H. Wiedersich, J. Nuc. Mat. 80 (1979), 172-179.

13. A. D. Marwick, R. C. Piller, and P. M. Sivell, J. Nuc. Mat. 83 (1979), 35-41.

14. R. C. Piller and A. D. Marwick, J. Nuc. Mat. 83 (1979), 42-47.

15. R. A. Johnson and N. Q. Lam, Phys. Rev. B. 13 (1976), 4364-4375.

16. A. D. Marwick, J. Phys. F, Metal Phys. 8, No. 9, (1978), 1849-1861.

17. P. R. Okamoto and H. Wiedersich, J. Nuc. Mat. 53 (1974), 336-45.

18. H. W. King, J. Mat. Sci. 1 (1966), 79-90.

19. P. Wilkes, Acta. Met. 16 (1968), 153.

20. H. V. Smith and R.G. Lott, Nuc. Inst. Methods 143 (1977), 125-132.

21. D. K. Brice, SAND 75-0622, Sandia Laboratories, Albuquerque, NM, July 1977.

22. L. E. Davis, N. C. MacDonald, P. W. Palmburg, G. E. Riach, and R. E. Weber, Handbook of Auger Electron Spectroscopy, Physical Electronic Industries, Inc.

23. P. M. Hall, J. M. Morabito, and D. K. Conley, Surface Science 62 (1977), 1-20.

24. P. M. Hall and J. M. Morabito, Surface Science 67 (1977), 373-392.

25. M. Suleman and E. B. Pattinson, J. Physics F, Metal Physics 1 (1971), L24-L27; also J. Physics F: Metal Physics 3 (1973), 497-504.

26. R. Buhl, W. K. Huber, and E. Lobach, Proc. 2nd Intl. Conf. on Solid Surfaces, 1974, in Japan J. Appl. Phys. Suppl. 2, Pt. 2, (1974), 807-810.

27. T. Koshikawa and R. Shimizu, Phys. Letters 44A(2) (1973), 112-113.

28. A. Bartels, F. Dworschak, H. P. Meurer, C. Abromeit, and H. Wollenberger, J. Nuc. Mat. 83 (1979), 24-34.

29. T. Takeyama, S. Ohnuki, H. Takahashi, Electron Microscopy 1980, Vol. 4, 208-212.

30. T. Takeyama, S. Ohnuki, H. Takahashi, J. Nucl. Mat. 89 (1980), 253-262.

31. A. J. Bradley and H. J. Goldschmidt, J. Inst. Metals 2 (1939), 389-401.

32. T. S. Hutchison and J. Reekie, Phys. Rev. 83 (1951), 854-855.

33. E. T. Teatum, et al., LA-4003, (1968).

34. A. G. H. Anderson and A. W. Kingsbury, Trans. AIME 152 (1943), 38-47.

35. W. Klement, Trans. AIME 233 (1965), 1180-1182.

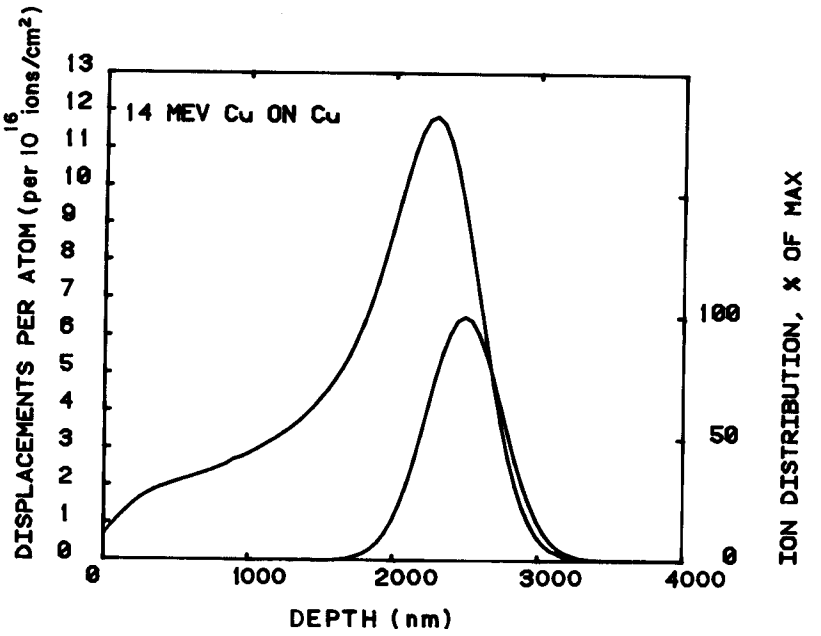

Figure 1. Energy deposition profile, in displacements-per-atom (dpa), for 14 MeV Cu ions incident on a Cu target, normalized for 10^{16} ions/cm^2. (Generated using Brice code [21]).

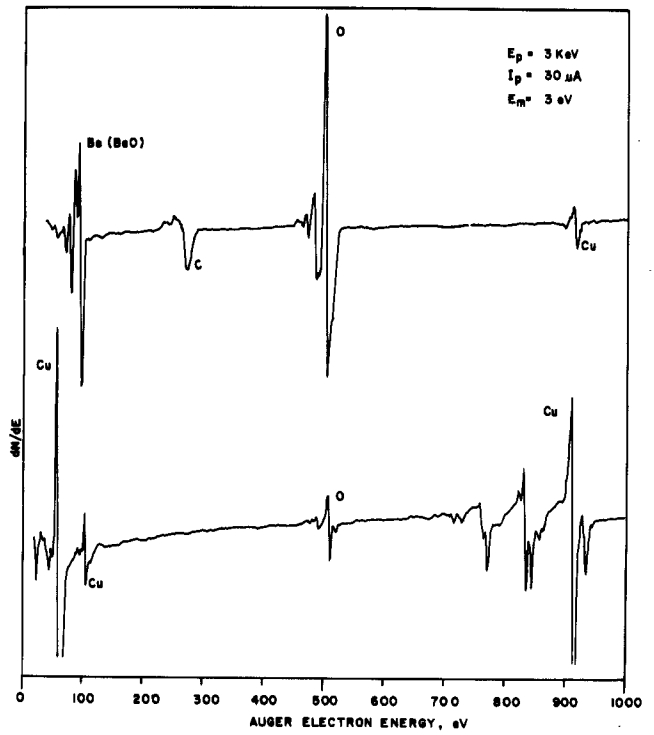

Figure 2. Typical Auger electron spectra for irradiated Cu-3.4 at % Be. Top: irradiated surface before sputtering. Bottom: after sputtering until alloy composition no longer changes with depth (~ 100 nm depth).

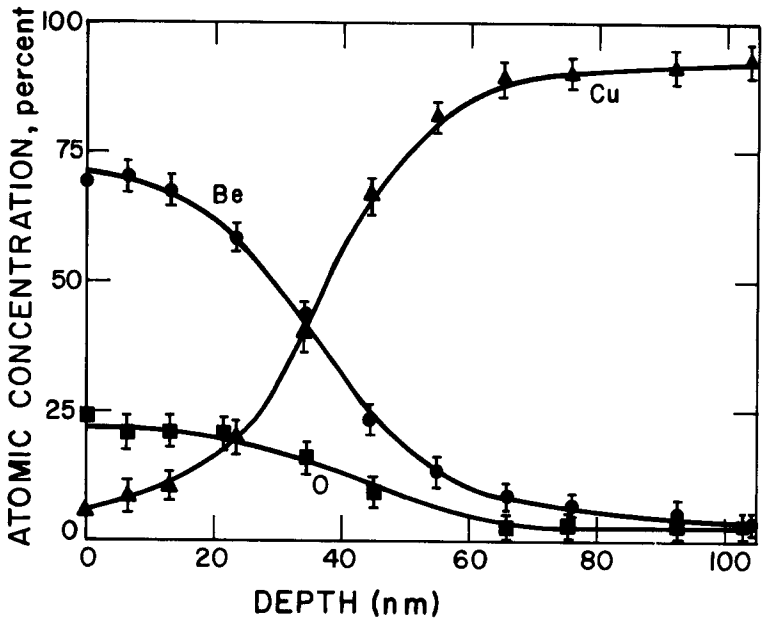

Figure 3. Concentration vs. depth profiles of Be, Cu and oxygen in Cu-3.4 at % Be irradiated with 1.8 x 10^{16} ions/cm^2 (1.3 surface dpa) at 475°C. These concentration profiles are first order approximations, generated from Auger electron spectroscopy data.

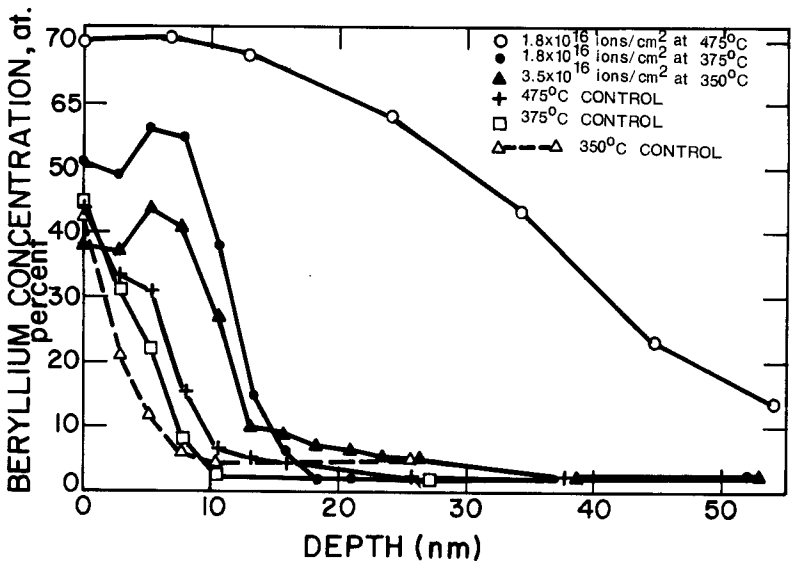

Figure 4. Concentration vs. depth profiles of Be in Cu-3.4 at % Be irradiated at 475°C (1.3 surface dpa), 375°C (1.3 surface dpa), and 350°C (2.6 surface dpa), generated from AES data. Control measurements were obtained from areas of the specimens masked from the Cu ion beam.

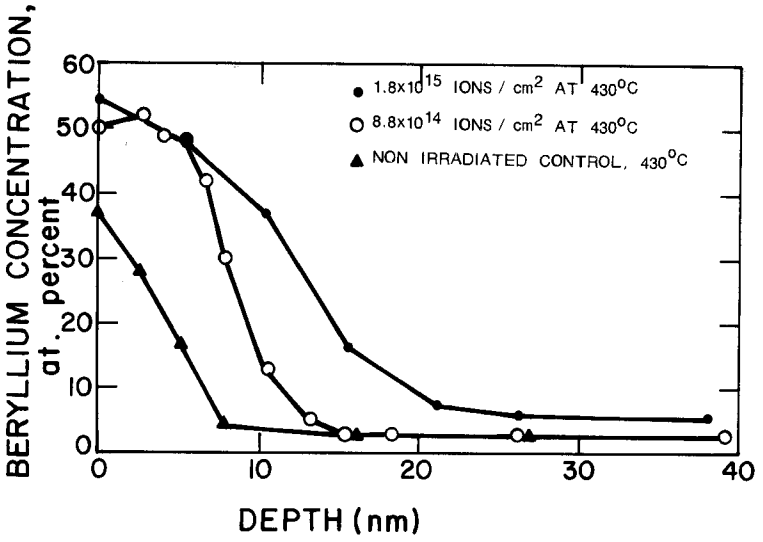

Figure 5. Beryllium concentration vs. depth profiles in Cu-3.4 at % Be irradiated at 430°C to relatively low doses (0.13 and 0.06 surface dpa). Concentrations are first-order approximations generated from AES data.

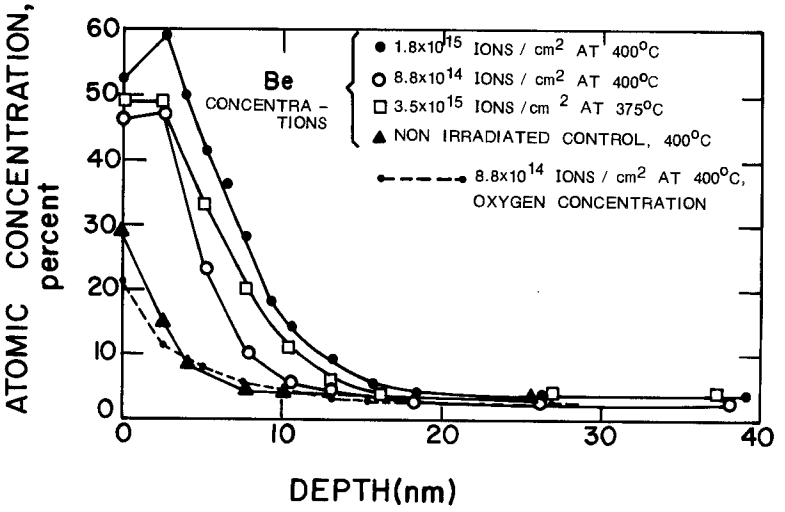

Figure 6. Concentration vs. depth profiles in Cu-3.4 at % Be irradiated at 400°C to relatively low doses (0.13 and 0.06 surface dpa), and at 375°C (0.25 surface dpa). The oxygen profile shown here is typical of these specimens. Concentrations are first order approximations generated from AES data.

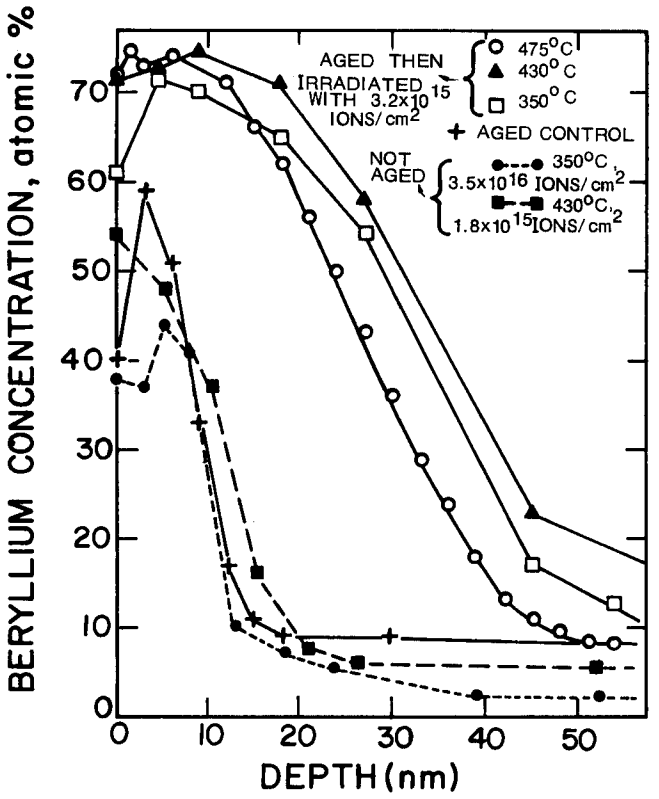

Figure 7. Comparison of Be concentration profiles in Cu-3.4 at % Be specimens aged before irradiation, with Be profiles in specimens heated only during irradiation. The 475°C and 430°C aged specimens were also heated after irradiation (see text for details).

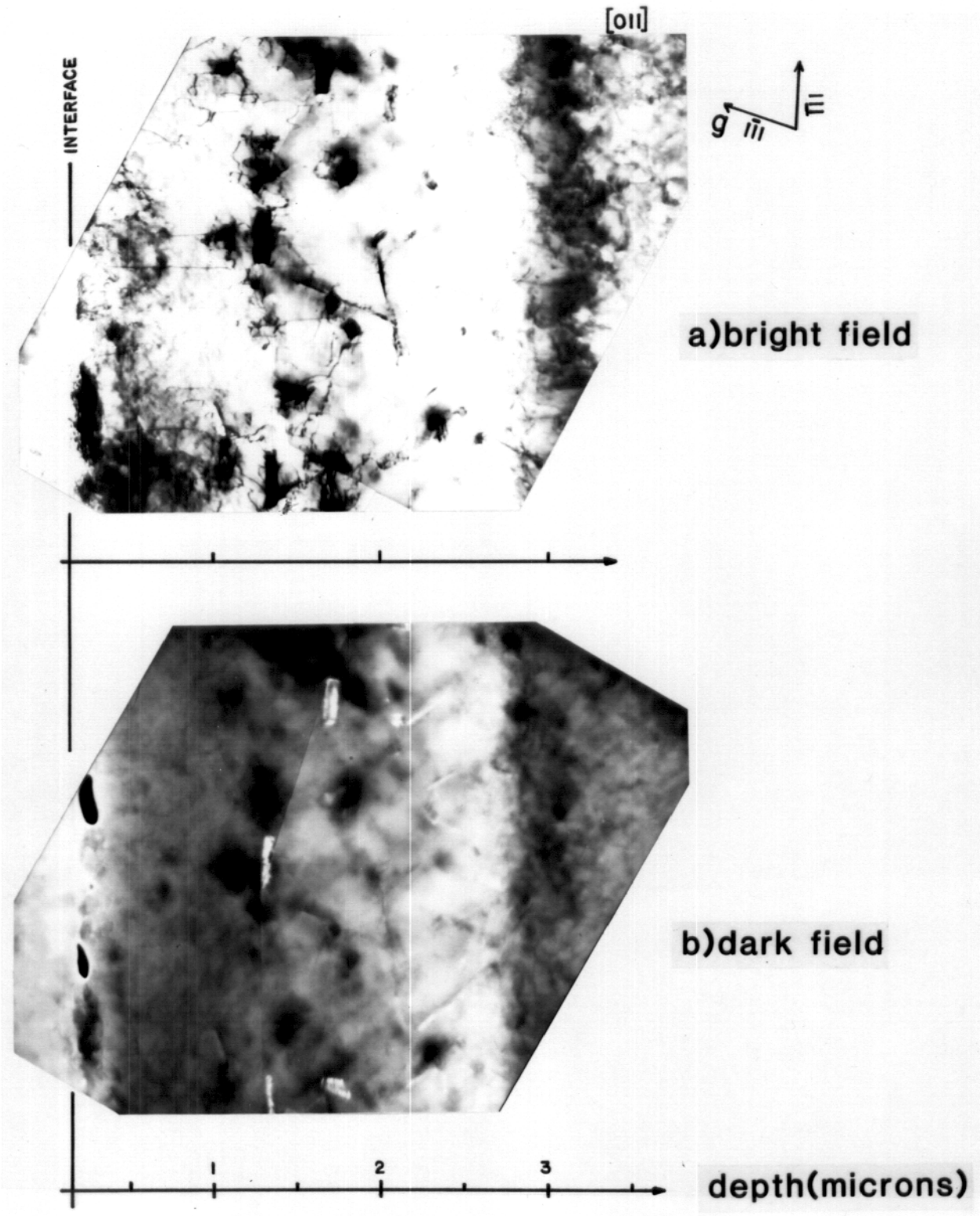

Figure 8. Electron-micrographs of irradiation-induced precipitation in Cu-3.4 at % Be irradiated at 430°C with 3.2 x 10^{15} ions/cm^2 (0.26 surface dpa). The damage zone, which extends to a depth of ~ 3 microns, is shown here in cross section. A precipitate reflection was used for the dark field image. Note the absence of precipitation beyond the damage zone.

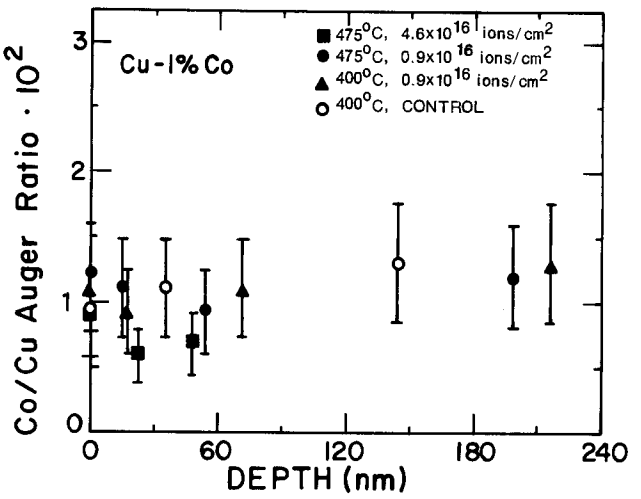

Figure 9. Relative cobalt concentration vs. depth profiles in Cu-1 % Co irradiated at 475°C (3.5 and 0.7 surface dpa) and 400°C (0.7 surface dpa), generated from AES data.

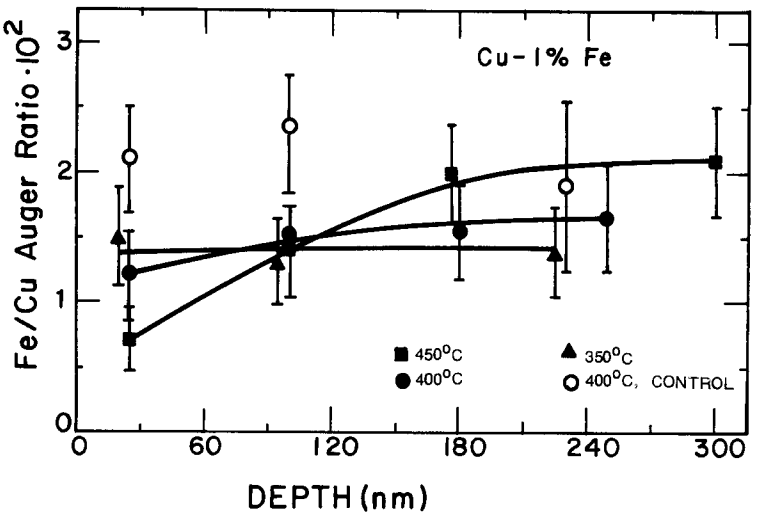

Figure 10. Relative iron concentration vs. depth profiles in Cu-1% Fe specimens irradiated with 1.1 x 10^{16} ions/cm^2 (0.83 surface dpa) at 450°C, 400°C, and 350°C.